Nanoscale Advances



PAPER

View Article Online
View Journal | View Issue



Cite this: Nanoscale Adv., 2024, 6, 1480

Kinematics of electromigration-driven sliding of Co nanorod fillers inside multi-walled carbon nanotubes†

Kensuke Adachi, a Shoqo Matsuyama, a Yuki Sakai and Hideo Kohno b *bc

The movement of Co nanorods driven by electromigration inside multi-walled carbon nanotubes was observed using *in situ* transmission electron microscopy. This study provides a unique method of experimental determination of both the electromigration force strength and sliding friction. When the tip of a biased electrode was located within the portion of a Co nanorod filler and an electric current was applied to push a part of the Co filler along the flow of electrons, the Co filler showed a trigonometric motion. Both the electromigration force strength and sliding friction were determined by analysis of the trigonometric movements. When a reversed electric current was applied to pull a part of the Co nanorod filler, its motion was hyperbolic-cosine like, and the motion was not suitable to determine the strengths of the two forces. Our method and the results would be useful for the development of the methods to precisely control mass transfer at the nanoscale.

Received 26th December 2023 Accepted 6th February 2024

DOI: 10.1039/d3na01149f

rsc.li/nanoscale-advances

1 Introduction

Electromigration is a well-known phenomenon in which the transport of atoms occurs in metals under high current density. ¹⁻⁶ Electrons traveling along the opposite direction of the applied electric current exchange their momentum with metal atoms that compose the conductive wires. As a result, the metal atoms are forced to move in the direction of the flow of electrons. This phenomenon has been studied intensively because electromigration is a cause of integrated circuit failure. ⁷⁻¹¹

The development of methods for mass transport at the nanoscale is important; in addition to the utilization of thermal gradients, i.a., the direction of transport can be easily controlled, *i.e.*, the direction of mass transport is along the flow of electrons, the electron wind force. It should be noted that an entire nano-object can be moved through the use of electromigration, while only atoms/ions move with macroscopic electromigration. The electromigration of nanomaterials inside carbon nanotubes (CNTs) has been studied using *in situ* transmission electron microscopy (TEM) and scanning electron

microscopy (SEM). Various materials such as Ni¹⁵ and Te¹⁶ can be encapsulated inside CNTs, and these materials can move inside the CNTs by the force of electromigration. CNTs as hosts are also suitable for *in situ* observations due to their thin walls. Electromigration has been used to develop nanopipettes,¹⁷ and the nanoscale printing of metal on graphite using the electromigration of metal in CNTs has also been reported.¹⁸

To control the movement of nano-objects driven by electromigration, it is essential to estimate the magnitude of the electron wind force acting on the moving nano-objects. Electron wind force has been investigated theoretically by several groups. 19-26 To estimate the magnitude of the force of electromigration, theoretically calculated or assumed values have been used for effective valences. 16 In addition to the magnitude of the force of electromigration, it is also necessary to determine the magnitude of kinetic friction to understand and control the movement of nano-objects. This study provides a method for experimental determination of the magnitudes of sliding friction and the force of electromigration for moving metal nano-objects inside multi-walled carbon nanotubes (MWCNTs). The motion of Co nanorods inside MWCNTs was observed using TEM and analyzed in terms of classical kinematics.

^aDepartment of Engineering, Graduate School of Engineering, Kochi University of Technology, Kami, Kochi 782-8502, Japan

2 Experimental

MWCNTs with Co nanorods were fabricated as follows. An alumina substrate with a 30 nm-thick Co deposition was sealed in an evacuated silica tube with 3 mg of a mixture of graphite powder, palmitic acid, and saccharin at a weight ratio of 664: 86:1. The sample was then heated to 1100 °C for 20 min to induce nanotube growth. Au nanoparticles were deposited on

^bSchool of Engineering Science, Kochi University of Technology, Kami, Kochi 782-8502, Japan. E-mail: kohno.hideo@kochi-tech.ac.jp; Fax: +81-887-57-2520; Tel: +81-887-57-2506

Center for Nanotechnology, Kochi University of Technology, Kami, Kochi 782-8502, Japan

[†] Electronic supplementary information (ESI) available: Movies SM1-3. See DOI: https://doi.org/10.1039/d3na01149f

the surfaces of the grown MWCNTs to examine Joule heating. The grown MWCNTs were mounted on Cu or Au wires for TEM (JEOL ARM200F, operated at 200 kV) observations. TEM images and movies were obtained using TVIPS XF416 or Gatan Rio16 CCD cameras with a resolution of 1024×1024 at 10 or 25 fps. A source measure unit (Yokogawa GS610) was used to apply voltage and current. W or Ni needles were used as biased probes. For electromigration experiments, we selected MWCNTs with a straight and homogeneous inner diameter without inclusions other than aimed Co fillers.

Results and discussion

Fig. 1 shows the results of TEM characterization of the Co nanorod fillers. The electron diffraction pattern was consistent with that of twinned face-centered cubic (fcc) Co crystals with the twin boundary along the axis of the nanorod. Two other Co nanorods were also examined and confirmed to be twinned. Energy-dispersive X-ray spectroscopy (EDX) analysis also confirmed that the nanorod fillers were Co. Co was used as a catalyst for the growth of MWCNTs, and it is likely that Co was taken into the inner spaces of the grown MWCNTs. The fcc phase of Co is stable above 417 °C, and the Co crystals of the fcc phase would have been quenched during the cooling process of nanotube growth.

In the first experiment, the micro-probe was located at an intermediate position of a nanorod filler in a MWCNT, as indicated by the blue arrow in Fig. 2(a). The right end of the MWCNT was connected to a grounded Cu supporting wire. The nanorod filler was approximately 470 nm long and 16 nm in

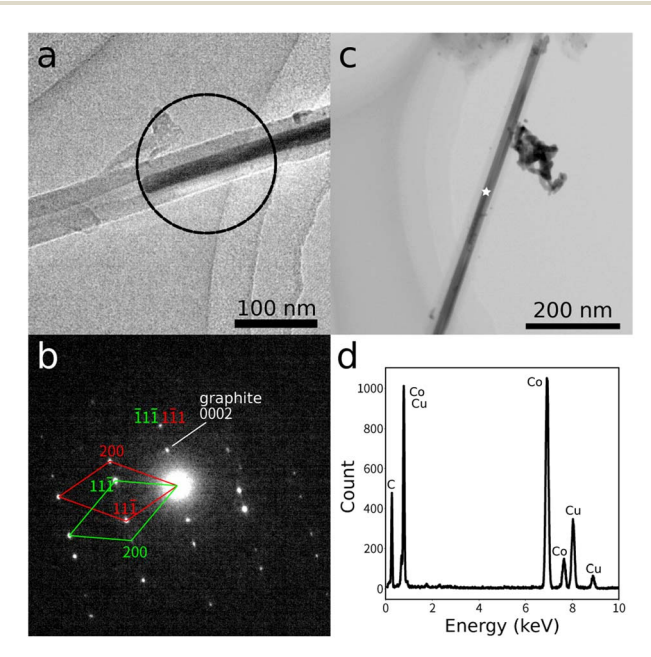
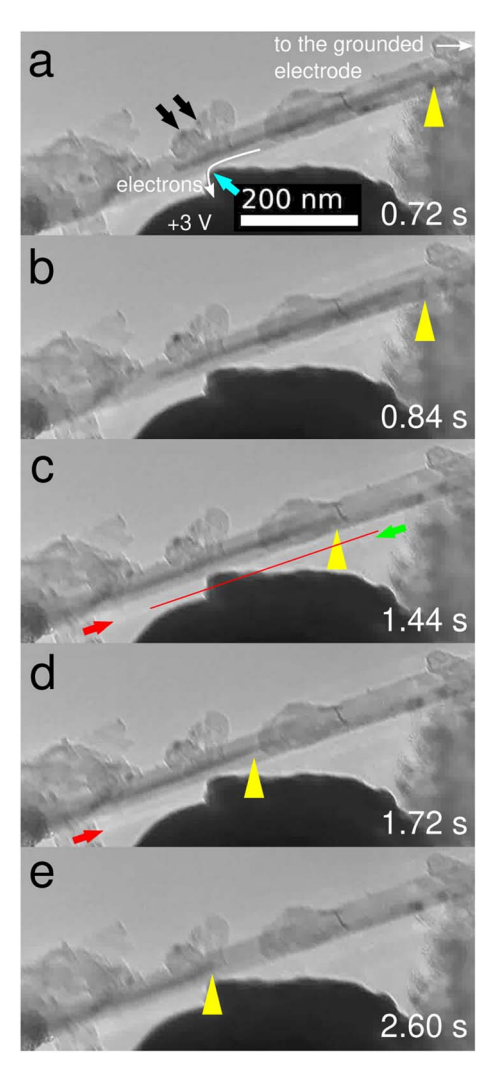


Fig. 1 (a) TEM image of a MWCNT with a Co nanorod filler. (b) Electron diffraction pattern obtained from the region marked with the circle in (a). The diffraction pattern was from a twinned crystal, and is marked with red and green. (c) TEM image of another MWCNT with a Co filler. (d) EDX spectrum measured from the point marked with a star in (c). The Cu peaks were from the TEM microgrid.



In situ TEM observation of the movement of a Co nanorod inside a MWCNT (snapshots from ESI Movie SM1†). The right-hand part shows the MWCNT containing a filler Co nanorod and connected to the grounded electrode. The probe was located within the portion with the Co filler (blue arrow in (a)). When the probe was positively biased, the Co filler moved to the left (a-d), then stopped when its right end came close to the probe (e). The yellow arrowheads indicate the position of the right end of the Co filler. The red line and red arrows indicate the position of a white line due to the diffraction contrast of the Co filler, while the green arrow indicates the position of the diffraction contrast from the MWCNT. The time was measured from the start of the ESI Movie SM1.†

diameter. The host MWCNT was approximately 56 nm in diameter and its wall was approximately 20 nm thick. The length between the probe contact position and the right end of the nanorod filler was initially ca. 420 nm. The nanorod filler was stationary before application of the electric current. When a positive bias potential of 3 V was applied to the micro-probe, electrons flew through the MWCNT and the nanorod filler from the right to the left toward the probe contact, and the nanorod filler then began to move left along the direction of the accelerating electron wind force (Fig. 2(b)-(d)). When the right end of the nanorod filler came close to the probe contact, the nanorod filler decelerated and then stopped (Fig. 2(e); see ESI Movie

SM1†). It was noted that the electric current did not flow in the portion that was located to the left of the probe contact. The intensity of the electric current was not recorded for this experiment.

Two Au nanoparticles [indicated by the black arrows Fig. 2(a)] were located on the surface of the MWCNT near the probe contact to examine the effect of Joule heating. These Au nanoparticles did not shrink during the experiment, which indicates that the temperature of the MWCNT and the nanorod filler was below the boiling point of Au (2700 °C). It has been well-known that the melting point of nanoparticles depends on their size, and it is lower than that of the bulk crystal.27 It is expected that a boiling point of a material would behave similarly. Accordingly, the boiling point of the Au nanoparticles would have been lower than that of the bulk crystal. A white line was observed outside the MWCNT/nanorod, as shown by the red arrows in Fig. 2(c) and (d), which was due to the diffraction contrast from the nanorod filler. The position of the white line was different from the diffraction contrast from the MWCNT (indicated by the green arrow in Fig. 2(c)), and the white line moved with the nanorod filler. This is evidence that the filler nanorod was solid and the sample temperature was below the melting point of Co (1495 °C). Furthermore, in our previous study, it was found that Au nanoparticles on the surface of a MWCNT shrank and disappeared at 1000 °C within a couple of seconds if without the Leidenfrost effect; therefore, it was most likely that the sample temperature was below 1000 °C.

Fig. 3 shows a plot of the movement distance as a function of time. The plot shows that the nanorod filler initially accelerated and then decelerated. This behavior appears to be trigonometric. Here we discuss the kinematics of the observed behavior. The equation of motion of the nanorod filler inside the MWCNT is given by:

$$m\frac{\mathrm{d}^2x}{\mathrm{d}t^2} = \alpha(L-x) - f,\tag{1}$$

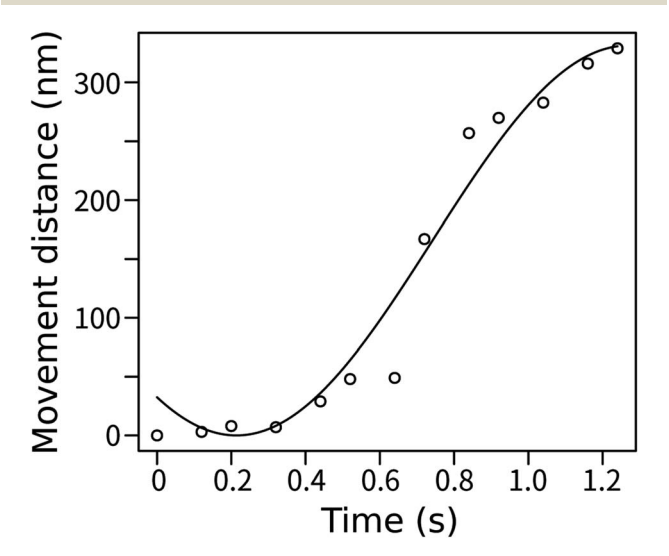


Fig. 3 Plot of the movement distance as a function of time. The solid line is the fitted function.

where m is the mass of the moving nanorod filler, α is the strength of the force of electromigration per unit length, x is the position of the right end of the nanorod filler measured from its initial position along the path of the movement, L is the initial length between the electrical contact and the right end of the nanorod filler, and f is the sliding friction. This equation applies only for $0 \le x \le L$. Only the portion of the nanorod filler between its right end and the electrical contact with the probe receives the force of electromigration, whereas the entire nanorod filler is subject to sliding friction. The sum of these two forces determines the magnitude of acceleration of the nanorod filler. Given that the sliding friction is constant and the initial velocity is zero, the following trigonometric solution is obtained:

$$x(t) = \left(L - \frac{f}{\alpha}\right)(1 - \cos \omega t),\tag{2}$$

$$\omega = \sqrt{\frac{\alpha}{m}}. (3)$$

The fitting curve for the experimental data with this function is plotted as a solid line in Fig. 3. The result of the fitting supports our simple model. Given that the nanorod filler was composed of Co, its mass was estimated to be approximately 8.4 \times 10⁻¹⁹ [kg]. Therefore, we obtain $\alpha = 7.4 \times 10^{-27}$ [N nm⁻¹] and $f = 1.9 \times 10^{-24}$ [N]. The strength of the sliding friction per nanometer is determined to be 4.0×10^{-27} [N nm⁻¹].

If we deal with the motion of a nanorod filler that moves simply between two electrodes, then its equation of motion is:

$$m\frac{\mathrm{d}^2x}{\mathrm{d}t^2} = \alpha L_{\text{whole}} - f,\tag{4}$$

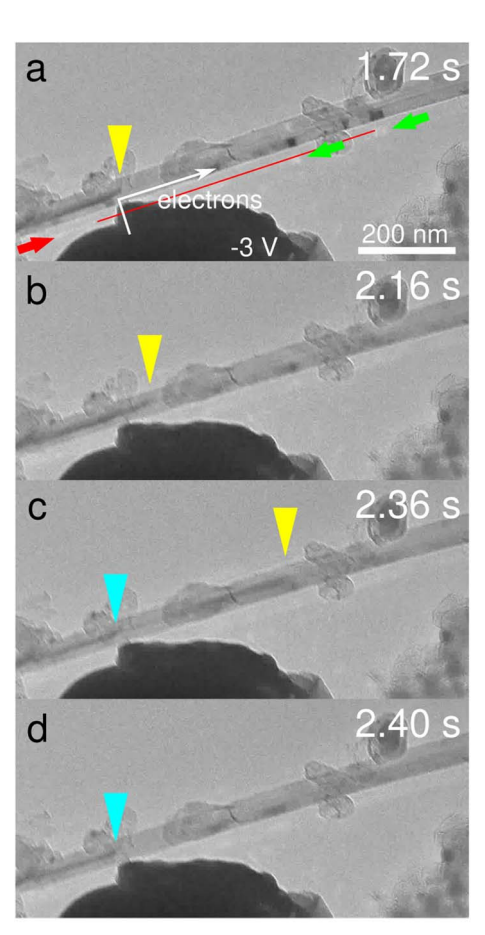
where $L_{\rm whole}$ is the entire length of the nanorod filler. In this case, we can determine only the total strength of the two forces, whereas we could determine each strength of the forces if the probe was located between the two ends of the filler and a fraction of the filler was pushed against the other fraction, as shown in Fig. 2.

After the operation shown in Fig. 2, the motion of the nanorod filler was observed with the application of a reversed electrical potential of -3 V to the micro-probe, as shown in Fig. 4(a)–(d) and ESI Movie SM2.† In this case, a fraction of the nanorod filler between its right end and the electrical contact was pulled to the right along the electron wind force. When the electric voltage was applied, the filler began to move toward the grounded electrode. The filler then fragmented into two pieces at the electric contact, and the right fragment kept moving right, while the left fragment stopped; the right fragment was torn from the rest because the fragment of the nanorod filler between its left end and the electric contact did not receive electromigration, and was only pulled to the left by the sliding friction.

The motion of the nanorod filler before fragmentation is plotted in Fig. 4(e). The plot appeared to be quadratic. In this case, the equation of motion is:

$$m\frac{\mathrm{d}^2x}{\mathrm{d}t^2} = \alpha x - f,\tag{5}$$

Paper



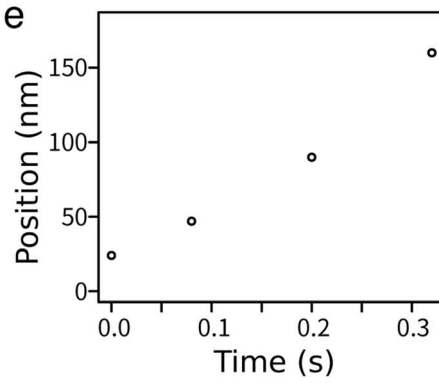


Fig. 4 (a-d) In situ TEM observation of the movement of the Co nanorod filler in the MWCNT (snapshots from ESI Movie SM2†) after the movement shown in Fig. 2. The probe was negatively biased, and the Co nanorod filler moved to the right (a and b). The position of the right end of the Co nanorod filler is indicated with yellow arrowheads. The Co filler nanorod was split into two at the position indicated by the blue arrowhead (c). Finally, the right part moved out of sight, while the left part of the Co filler did not move (d). (e) Plot of the position of the right end of the Co filler before splitting into two parts, as measured from the contact between the probe and the MWCNT.

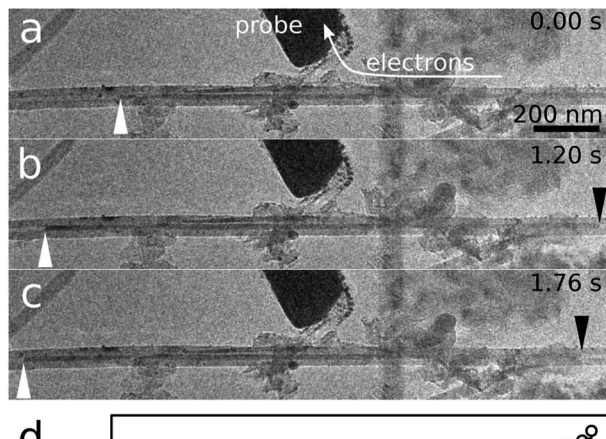
where *x* is the position of the right end of the filler measured from the position of the electrical contact at the right. Under the conditions of $x(0) = x_0$ and $\dot{x}(0) = 0$, we obtain

$$x(t) = \left(x_0 - \frac{f}{\alpha}\right) \cosh(\omega t) + \frac{f}{\alpha} \tag{6}$$

$$x(t) \simeq A(\omega t)^2 + B. \tag{7}$$

The second-order Taylor expansion shows that the behavior is almost quadratic, which indicates that it is difficult to estimate parameters by fitting with a hyperbolic cosine function because the scaling in t is almost equivalent with that in x. We were not able to estimate the strengths of the forces for this case due to poor convergence in the optimization of the parameters. We note that the experimental data were well fitted with the quadratic function.

We performed another experiment that was the same as that shown in Fig. 2 in which the constant-current mode was used and an electric current of 70 µA was applied and the results are shown in Fig. 5 and ESI Movie SM3.† Initially, the Co nanorod filler was not moving because an electric current was not applied. When an electric current was applied, the MWCNT showed a twitch, and the Co nanorod filler started moving. The Co nanorod kept moving during the electric current application. When the electric current was stopped, the MWCNT



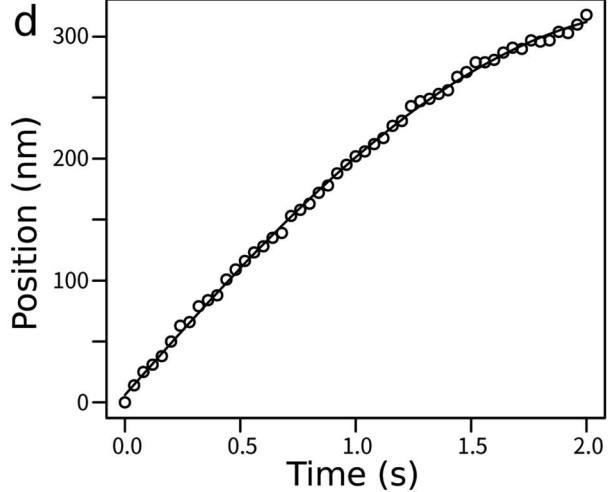


Fig. 5 (a-c) In situ TEM observation of the movement of a Co filler inside a MWCNT (second example, snapshots from the ESI Movie SM3†). The probe was positively biased, and the Co nanorod moved to the left. The left and right ends of the Co nanorod are indicated by the white and black arrowheads, respectively. (d) Plot of the movement distance of the Co nanorod as a function of time. The solid line is the fitted function.

showed a twitch again, and the Co nanorod filler stopped moving. This clearly indicates that the applied electric current was the driving force of the motion of the Co nanorod. The nanorod filler was 18 nm in diameter and 1700 nm long with an estimated mass of 3.8 \times 10 $^{-18}$ [kg]. The host MWCNT was approximately 56 nm in diameter. The current density in the Co nanorod filler was estimated to be ca. 0.26 μA nm $^{-2}$ using the reported values of resistivity, 9.8 \times 10 $^{-6}$ and 6.24 \times 10 $^{-8}$ [Ohm m] for graphite (perpendicular to the c-axis) 28 and Co, 29 respectively, and the dimensions of the nanorod filler and the MWCNT. The function 2 was fitted with the experimental data to obtain $\alpha = 1.4 \times 10^{-27}$ [N nm $^{-1}$] and $f = 1.1 \times 10^{-24}$ [N]. The amplitude of the sliding friction per nanometer was estimated to be 6.3×10^{-28} [N nm $^{-1}$].

Co nanorods have never moved inside NWCNTs without applying an electric current in our observations. In addition, cantilevered tubes with Co fillers did not show bending during TEM observation. Accordingly, the magnetic force working on the Co fillers in the TEM must have been negligible. We speculate that the magnetic force would have had only a very small contribution to the normal force at the filler/nanotube interface.

Electromigration of a Co nanorod filler without the TEM electron beam was also examined as shown in Fig. 6. An electric current of 0.19 mA was applied for 2.55 s under the electron-beam blanking condition. The direction of the flow of electrons was from right to left. After the application of the electric current, the position of the Co nanorod filler was moved to the left along the direction of direction of the flow of electrons. The result shows that the electromigration motion of the Co nanorod filler occurred without the irradiation of TEM electrons.

The strength of the electromigration force should be proportional to the current density. At this moment, we cannot compare the two values of the electromigration forces between the two experiments obtained in this study, because the current density is unknown for the first experiment. The strength of sliding friction would be the product of dynamic friction coefficient, contact area, and pressure at the interface between

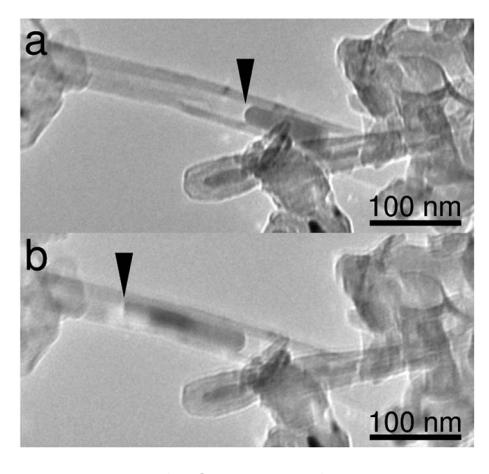


Fig. 6 Electromigration of a Co nanorod filler without the TEM electron beam: (a) before and (b) after electromigration (0.19 mA, 2.55 s).

a filler and a MWCNT. The amplitude of the sliding friction and the diameter of the filler was $4.0 \times 10^{-27} \, [\mathrm{N} \ \mathrm{nm}^{-1}]$ and 16 nm for the first example, respectively, while they were $6.3 \times 10^{-28} \, [\mathrm{N} \ \mathrm{nm}^{-1}]$ and 18 nm for the second example, respectively. The values of the strength of the sliding friction were different by one order of magnitude, while the diameters were similar. This suggests that the amplitude of sliding friction depends on other factors, such as temperature. Further studies are necessary to compare our results with other experimental works on nanoscale sliding friction. ³⁰

4 Conclusions

In conclusion, we have developed a method to estimate the strengths of the force of electromigration and the sliding friction on nanorod fillers moving inside MWCNTs. If one electrode was located between the two edges of a nanorod filler and the electron wind force was applied to one portion to push the other portion, then the strengths of the two forces could be easily estimated. Conversely, it is difficult to estimate these strengths when the nanorod filler is pulled. We expect these results will be useful to inspect theories for estimation of the strengths of the forces of nanoscale electromigration and sliding friction, and for the development of methods to control transfer precisely mass using nanoscale electromigration.

Conflicts of interest

There are no conflicts to declare.

References

- 1 H. Huntington and A. Grone, *J. Phys. Chem. Solids*, 1961, **20**, 76–87.
- 2 J. R. Black, IEEE Trans. Electron Devices, 1969, 16, 338-347.
- 3 I. Blech and E. Meieran, J. Appl. Phys., 1969, 40, 485-491.
- 4 C.-K. Hu, R. Rosenberg and K. Lee, *Appl. Phys. Lett.*, 1999, 74, 2945–2947.
- 5 I. A. Blech, J. Appl. Phys., 1976, 47, 1203-1208.
- 6 H. Park, A. K. Lim, A. P. Alivisatos, J. Park and P. L. McEuen, Appl. Phys. Lett., 1999, 75, 301–303.
- 7 J. Lloyd, J. Appl. Phys., 1991, 69, 7601-7604.
- 8 K.-N. Tu, J. Appl. Phys., 2003, 94, 5451-5473.
- D. Young and A. Christou, *IEEE Trans. Reliab.*, 1994, 43, 186– 192.
- 10 C. M. Tan and A. Roy, *Mater. Sci. Eng.*, R, 2007, 58, 1–75.
- 11 F. M. d'Heurle, Proc. IEEE, 1971, 59, 1409-1418.
- 12 B. Regan, S. Aloni, R. Ritchie, U. Dahmen and A. Zettl, *Nature*, 2004, **428**, 924–927.
- 13 J. Zhao, J.-Q. Huang, F. Wei and J. Zhu, *Nano Lett.*, 2010, **10**, 4309–4315.
- 14 M. Okada, D. Sasaki and H. Kohno, *Microscopy*, 2020, **69**, 291–297.
- 15 N. Kulshrestha, A. Misra and D. Misra, Nanotechnology, 2013, 24, 185201.

- 16 L.-B. He, L. Shangguan, Y.-T. Gao, S. Yang, Y.-T. Ran, Z.-Y. Lu, J.-H. Zhu, B.-J. Wang and L.-T. Sun, ACS Appl. Nano Mater., 2023, 7679-7685.
- 17 K. Svensson, H. Olin and E. Olsson, Phys. Rev. Lett., 2004, 93,
- 18 G. Melinte, S. Moldovan, C. Hirlimann, X. Liu, S. Bégin-Colin, D. Bégin, F. Banhart, C. Pham-Huu and O. Ersen, Nat. Commun., 2015, 6, 8071.
- 19 Y. W. Choi and M. L. Cohen, Phys. Rev. Lett., 2022, 129,
- 20 P. Rous and D. Bly, Phys. Rev. B: Condens. Matter Mater. Phys., 2000, 62, 8478.
- 21 J. Dekker, A. Lodder and J. Van Ek, Phys. Rev. B: Condens. Matter Mater. Phys., 1997, 56, 12167.
- 22 J. Dekker, P. Gumbsch, E. Arzt and A. Lodder, Phys. Rev. B: Condens. Matter Mater. Phys., 1999, 59, 7451.

- 23 J. Dekker and A. Lodder, J. Appl. Phys., 1998, 84, 1958-1962.
- 24 D. Kandel and E. Kaxiras, Phys. Rev. Lett., 1996, 76, 1114.
- 25 W. Wang, Z. Suo and T.-H. Hao, J. Appl. Phys., 1996, 79, 2394-2403.
- 26 R. S. Sorbello, Phys. Rev. B: Condens. Matter Mater. Phys., 1985, 31, 798.
- 27 P. Schlexer, A. B. Andersen, B. Sebok, I. Chorkendorff, J. Schiøtz and T. W. Hansen, Part. Part. Syst. Charact., 2019, 36, 1800480.
- 28 D. E. Gray et al., American Institute of Physics Handbook, 1972.
- 29 J. Speight, Lange's Handbook of Chemistry, McGraw-Hill Education, 2005.
- 30 M. R. Vazirisereshk, H. Ye, Z. Ye, A. Otero-De-La-Roza, M.-Q. Zhao, Z. Gao, A. C. Johnson, E. R. Johnson, R. W. Carpick and A. Martini, Nano Lett., 2019, 19, 5496-5505.